Pseudogap in electron-doped superconducting Sm$_{2-x}$Ce$_x$CuO$_{4-\delta}$ by interlayer magnetotransport

Tsuyoshi Kawakami,* Takasada Shibauchi,† Yuhki Terao, and Minoru Suzuki

Department of Electronic Science and Engineering, Kyoto University, Kyotodaigaku-Katsura, Nishikyo-ku, Kyoto 615-8510, Japan
(Received 26 December 2005; revised manuscript received 6 September 2006; published 30 October 2006)

c-axis interlayer magnetoresistivity is measured for an electron-doped (n-type) superconducting cuprate Sm$_{2-x}$Ce$_x$CuO$_{4-\delta}$ with $x=0.14-0.16$ using 30 nm thick small mesa structures. A systematic doping dependence is observed in the negative interlayer magnetoresistance (MR) component, from which the pseudogap onset temperature T^* is determined as the negative MR appearance temperature. For a doping level close to the phase boundary between superconductivity and antiferromagnetism, a T^* of 48 K is observed. It is also found that T^* decreases systematically with increasing x but is still higher than T_c. For all the doping levels, the result represents features characteristic of hole-doped (p-type) cuprates in the overdoped region, suggesting that the phase diagrams for the pseudogap are primarily similar for both the n- and p-type cuprates.

PACS number(s): 74.25.Dw, 74.25.Fy, 74.50.+r, 74.72.Jt

I. INTRODUCTION

The pseudogap in cuprates manifests itself as an anomalous depression of the density of states (DOS) in the normal state.[1] Its origin and relevance to high-T_c superconductivity have not been understood sufficiently. In hole doped cuprates, the pseudogap is observed usually in the underdoped and optimally doped regions. Recently, it was known that it is observed even in the heavily overdoped region.[2,3] In electron-doped (n-type) cuprates (L_{2-x}Ce$_x$CuO$_{4-\delta}$, where L =Pr, Nd, Sm, or Eu), on the other hand, the pseudogap was observed in a number of experiments.[4–14] In these measurements, the pseudogap was observed in two different energy scales. Angle-resolved photoemission spectroscopy (ARPES) measurements[4,5] on Nd$_{1.85}$Ce$_{0.15}$CuO$_4$ (NCCO) revealed that the pseudogaplike feature exists near the intersection of the Fermi surface with the antiferromagnetic Brillouin zone boundary ("hot spots"). This is a high-energy pseudogap or a large pseudogap, which spans in a 100–400 meV range. This result was supported by optical measurements[6–8] and Raman scattering results.[9] The high energy scale pseudogap is observed usually in the nonsuperconducting antiferromagnetic phase ($x<0.14$).[6] With increasing doping, the pseudogap onset temperature T^* decreases rapidly and appears to vanish near $x=0.15$.

In the superconducting region ($0.14 \leqslant x \leqslant 0.175$ in the case of NCCO), the pseudogap was reported variously. Tunneling spectroscopy measurements[11,12] on La$_{2-x}$Ce$_x$CuO$_{4-y}$ and Pr$_{2-x}$Ce$_x$CuO$_{4-y}$ indicated the presence of a low-energy pseudogap at an energy of ~ 10 meV, i.e., a small pseudogap. There is, however, no consensus on the doping range in which the low energy scale pseudogap is observed. In an extreme case, the absence of the pseudogap was indicated in nuclear magnetic resonance experiments on Pr$_{0.91}$LaCe$_{0.09}$CuO$_{4-y}$ (Ref. 10). The experimental results on the low-energy pseudogap are thus confusing and often contradictory. In this paper, we report the low-energy pseudogap for n-type Sm$_{2-x}$Ce$_x$CuO$_{4-\delta}$ (SCCO) and its onset temperature T^* determined definitely from the c-axis interlayer magnetotransport with a stress on its doping and magnetic field dependences. The values obtained for T^* are larger than those from tunneling spectroscopy measurements, the reason

for which we argue is ascribed to the magnetic field dependence of the pseudogap. The results are compared with the generic phase diagram of the p-type cuprates and its similarity is discussed.

The inconsistency among experimental results on the low-energy pseudogap is thought to arise from different interpretations of the pseudogap in the presence of magnetic fields. In those experiments[10–12] in which magnetic fields of $H=13-15$ T were used, the pseudogap was assumed not to be altered much by the magnetic fields. However, this is not likely the case. In different tunneling spectroscopy measurements[13] on Nd$_{1.85}$Ce$_{0.15}$CuO$_{4-y}$ and Pr$_{1.85}$Ce$_{0.15}$CuO$_{4-y}$, the low-energy density of states (DOS) was found to increase in the presence of a magnetic field of 12–16 T, a field greater than the upper critical field H_{c2}. This implies that the pseudogap can vary under a magnetic field. Furthermore, it is recently demonstrated that the pseudogap can be suppressed by magnetic fields,[14] similarly to the case for p-type Bi$_2$Sr$_2$CaCu$_2$O$_{8+\delta}$ (BSCCO).[2] Thus the pseudogap depends on the magnetic field and it should be measured by taking into account the magnetic field dependence strictly.

In highly anisotropic n-type cuprates, such as p-type Bi-based cuprates, the interlayer (c axis) transport is thought to occur via tunneling. Then, it follows that the c axis resistivity ρ_c reflects the DOS at the Fermi level. Therefore, the measurement of ρ_c provides a means to probe the pseudogap state.[15] In p-type cuprates, the pseudogap onset temperature T^* is determined as the temperature T at which ρ_c starts to deviate upward from the linear T dependence.[15,16] In n-type cuprates, on the other hand, this method does not apply. This is because in n-type cuprates ρ_c is T dependent like $\rho_0 + AT^\beta$, where $1<\beta<2$, even in the c-axis direction similar to a transport involving electron-electron scattering in the Fermi liquid. This nonlinear T dependence makes it difficult to determine T^* from the ρ_c-T curve straightforwardly. It is known, however, that the upturn part of ρ_c shows negative magnetoresistance (MR) in overdoped BSCCO (Ref. 2). Therefore, in the present study, we determine T^* for n-type cuprates as the temperature below which the negative MR appears.

The most serious problem in the measurements of the interlayer transport properties in n-type cuprates is the exis-
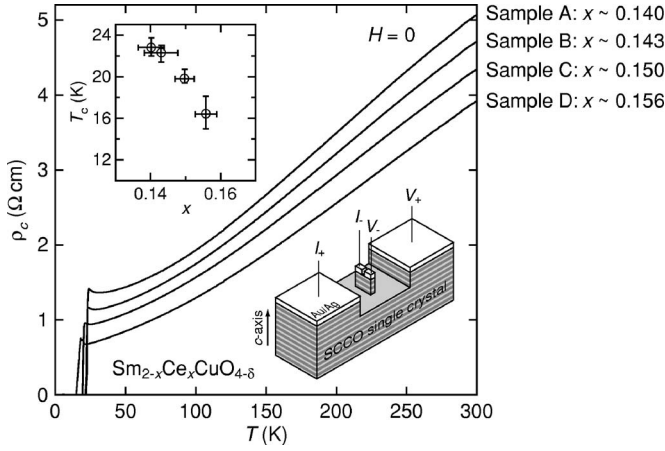
FIG. 1. T dependence of ρ_c for samples A–D with various x. Excitation current is 2 μA. Top-left inset: x dependence of T_c for the same samples. The vertical error bars for T_c indicate the transition width from the onset to the zero resistance. The superconducting onset temperature is defined as the temperature at which ρ_c reaches the peak. The horizontal error bars represent the standard deviation of the composition analysis. Bottom-right inset: Schematic illustration of the mesa structure in the present study (not to scale).

tence of the epitaxial stacking impurity phase,[17] which nucleates during the annealing process and hinders the accurate measurements of the intrinsic ρ_c. In order to circumvent this problem, we have fabricated small and thin mesa structures in which the impurity phase is absent. Using these small and thin mesa structures with various doping levels, we have measured the interlayer magnetotransport for the elucidation of the pseudogap in the n-type SCCO system. From the negative MR component observed, it is found that T^* decreases linearly with the carrier doping level, while it keeps a value greater than T_c in the whole x range observed. This finding demonstrates a similarity of the phase diagram between the p-type cuprates and the n-type SCCO system in the overdoped regime.

II. EXPERIMENT

SCCO single crystals were grown by the self-flux method[18,19] with a crucible-turnover technique to remove the solvent. We obtained single crystal plates 1–2 mm long and ~1 mm wide with flux-free shiny surfaces. As-grown crystals were annealed in flowing Ar at 945 °C for 15 h. The Ce concentration x was determined by energy dispersive x-ray spectroscopy analysis. In the analysis, more than six different points on a crystal surface were probed to give an averaged value. The analytical error for the value of x is less than 0.005. Using crystals with various x, small and thin mesa structures were fabricated on top of crystal surfaces with a standard photolithography and Ar ion milling technique.[15] From these mesas, we employed four samples with different x of ~0.140, 0.143, 0.150, and 0.156. These samples were labeled from A to D in order of increasing x. The mesas are approximately 2×10 μm^2 in horizontal area and 30 nm in height with two electrodes on the top. The mesa thickness is
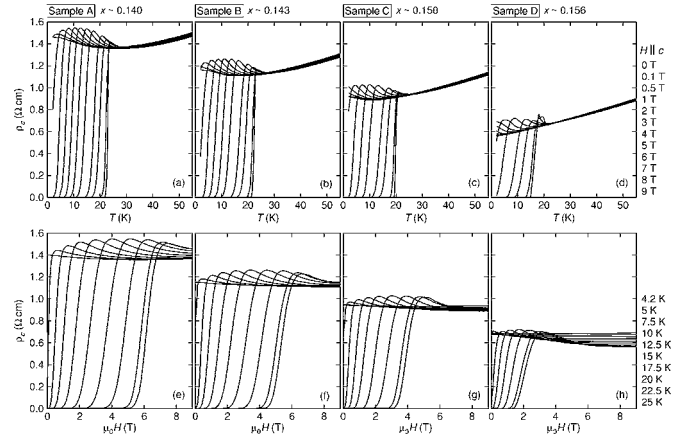

FIG. 2. (a)–(d) ρ_c-T curves for $H \| c$ for the SCCO mesas (samples A–D). (e)–(h) H dependences of ρ_c at various temperatures for $H \| c$ for the same samples.

much smaller than several hundred nm, a typical separation of the secondary phase stacking layers of 4–8 nm in thickness.[17] Because of a large resistivity anisotropy of ~10^4 for SCCO crystals, the four electrode configuration as illustrated in Fig. 1 is almost sufficient to provide intrinsic values for ρ_c. The error due to the dimensions is less than 5%.

III. RESULTS

Figure 1 shows the T dependence of ρ_c for samples A–D in the absence of a magnetic field. For all the samples, ρ_c exhibits metallic T dependence with the residual resistivity ratio more than twice that of SCCO bulk single crystals. The ρ_c of the mesas are less than 1/3 of that of the bulk crystals at low temperatures. This result demonstrates that the epitaxial secondary phase is absent in these samples. It is clearly seen in Fig. 1 that both T_c and ρ_c decrease with increasing x. The residual resistance is also reduced by a factor of ~0.5 with increasing doping from sample A–D. For sample D, the ρ_c-T curve just above the transition exhibits a small resistance peak, which vanishes immediately when a weak magnetic field is applied, as shown in Fig. 2(d). This behavior suggests that this anomalous peak results from a possible alteration of the current flow distribution when a part of surface has a little higher T_c, which might accidentally happen, and undergoes the superconducting transition. Even if such a layer is included as in sample D, the error involved in the magnitude of ρ_c is less than 10% as inferred from Fig. 2(d).

Figures 2(a)–2(d) show ρ_c-T curves for samples A–D in magnetic fields applied along the c axis, exhibiting a characteristic semiconductive upturn and a peak at $T = T_{peak}$ near the resistive transition. With increasing H, the upturn shows a systematic increase and a shift to lower temperatures, leading to a significant negative MR behavior in the lower T range. At high temperatures, on the other hand, the $\rho_c(T)$ shows a small positive MR. These field-dependent magnetoresistive behaviors, except the anomalous resistance peak for sample D, are attributable to the existence of the pseudogap for the same reason as in p-type BSCCO (Ref. 2). In particular, for sample D, the ρ_c-T curve exhibits a metallic behavior down
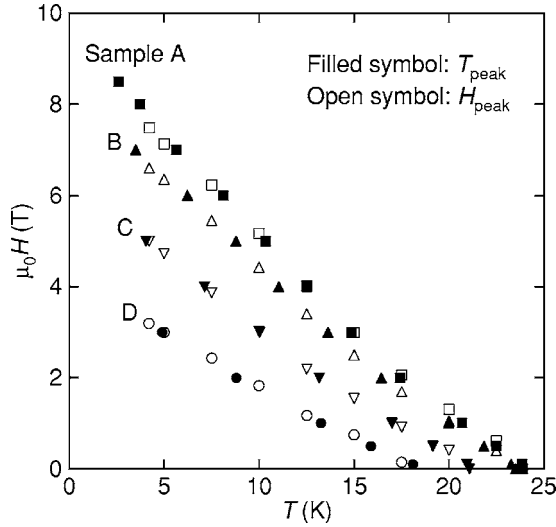
FIG. 3. Plots for $T_{\text{peak}}(H)$ (filled symbols) and $H_{\text{peak}}(T)$ (open symbols) for samples A–D in the H-T plane.

FIG. 4. (a) ρ_{cN}-T curves for samples A–D. The low temperature part of each curve is assumed to have the form $\rho_0 + AT^{\beta}$. Values for ρ_0, A, and β were determined for the calculated curve to fit the experimental ρ_c-T curve at $\mu_0 H = 9$ T. (b) T dependence of ρ_{cN} and ρ_{cPG} for sample A in the absence of a field. (c)–(f) H dependence of the estimated ρ_{cPG} values at various temperatures for samples A–D.

to 2 K for $\mu_0 H \geqslant 8$ T, implying that the pseudogap is almost entirely suppressed at a magnetic field of 8 T.

In Figs. 2(e)–2(h), the H dependence of ρ_c is shown at various temperatures for $H \| c$. Below T_c, all the ρ_c-T curves exhibit a peak at $H = H_{\text{peak}}$. The ρ_c-T curves at a temperature slightly above T_c show a negative MR behavior at low fields, which is partly or entirely counterbalanced by the positive MR component as H increases. At high T, the MR is positive and quadratic in H, as shown in the inset to Fig. 5(b).

Figure 3 shows plots both for H_{peak} vs T and for T_{peak} vs H in the H-T plane for samples A–D for the sake of comparison of the peaks in Fig. 2. For each sample, the plots for H_{peak} vs T and T_{peak} vs H coalesce on a single curve, which decreases almost linearly with increasing T and its slope decreases with increasing x. Thus H_{peak} decreases significantly with increasing x. If we take into account that H_{peak} is caused by the interplay between the MR effect of the pseudogap and the phase-fluctuation-induced resistive transition[20] and that it is a lower bound on H_{c2} (Ref. 21), the x dependence of H_{peak} may indicate that the coherence length ξ becomes longer with the doping in the SCCO system.

In order to determine the pseudogap temperature T^*, we use the formulation proposed in our previous paper,[14] i.e.,

$$\rho_c(T,H) = \rho_{cN}(T) + \rho_{cPG}(T,H) + \alpha(T)H^2, \quad (1)$$

where ρ_{cN} is the zero-field resistivity in the absence of the pseudogap, ρ_{cPG} is the extra resistivity component which emerges due to the evolution of the pseudogap, and α is the coefficient of the usual positive MR proportional to H^2. The value for α is obtained from the MR at high temperatures as is described later. This relationship is assumed to hold in the normal state. Since ρ_c is accompanied by both negative and positive MR, ρ_{cN} is unmeasurable below T^*. To estimate ρ_{cN}, the T dependence of ρ_{cN} below T^* is assumed to be $\rho_0 + AT^{\beta}$ in the presence of a high magnetic field.

The second term ρ_{cPG} produces negative MR. This term is also unmeasurable below T^* as in ρ_{cN}. If we assume ρ_{cN} as above so as to fit the extrapolation from higher temperatures,
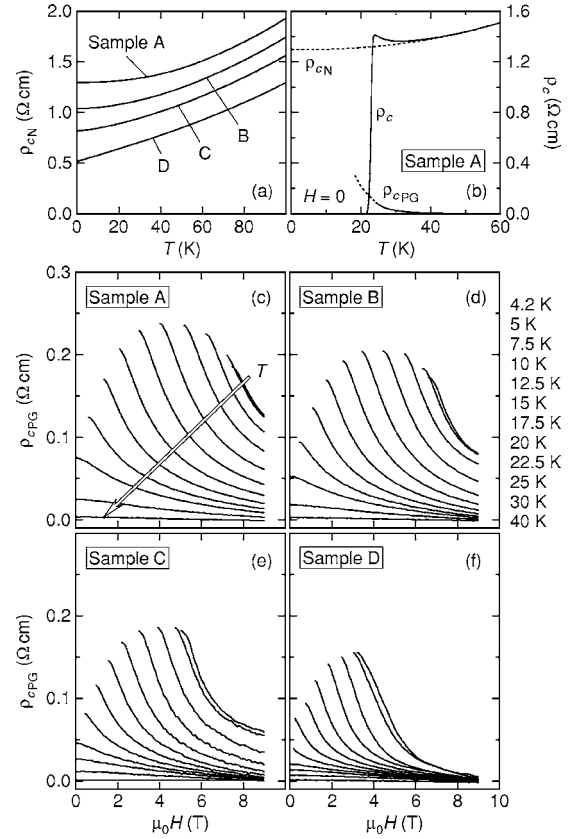
we can estimate ρ_{cPG} values by using Eq. (1). The T dependence for ρ_{cN} and its extrapolation to lower temperatures are shown in Fig. 4(a). Figure 4(b) displays the relationship between ρ_{cPG} and ρ_{cN} in the case of sample A. The estimates thus obtained for ρ_{cPG} are shown in Figs. 4(c)–4(f) as a function of both H and T for samples A–D. The result reveals a clear decrease in ρ_{cPG} with increasing doping. Moreover, rough extrapolation of $\rho_{cPG}(T,H)$ to $H=0$ and $T=0$ suggests that $\rho_{cPG}(0,0)$ is approximately one order of magnitude larger than $\rho_{cPG}(T_{\text{peak}},0)$. The value for $\rho_{cPG}(0,0)$ reflects the magnitude of the pseudogap. The results in Figs. 4(c)–4(f) indicate that the pseudogap magnitude decreases as x increases. This behavior is in close relation to T^*, which is evaluated in the following based on MR without any assumption for ρ_{cN}.

It is found that the ρ_c-H^2 relationship is linear in the T range higher than 50 K and that the T dependence for α is weak. Therefore, the coefficient α was determined from the linear ρ_c-H^2 relationship at 50 K and these values are used in the analysis which follows. The values for α are plotted in the inset to Fig. 5(d) as a function of x, showing an almost linear decrease with x. This significant decrease in α with x can be understood in terms of the modified Kohler's rule,[22] i.e., the relationship $\alpha \propto R_{H^2}/\rho(H=0)$, and a strong decrease
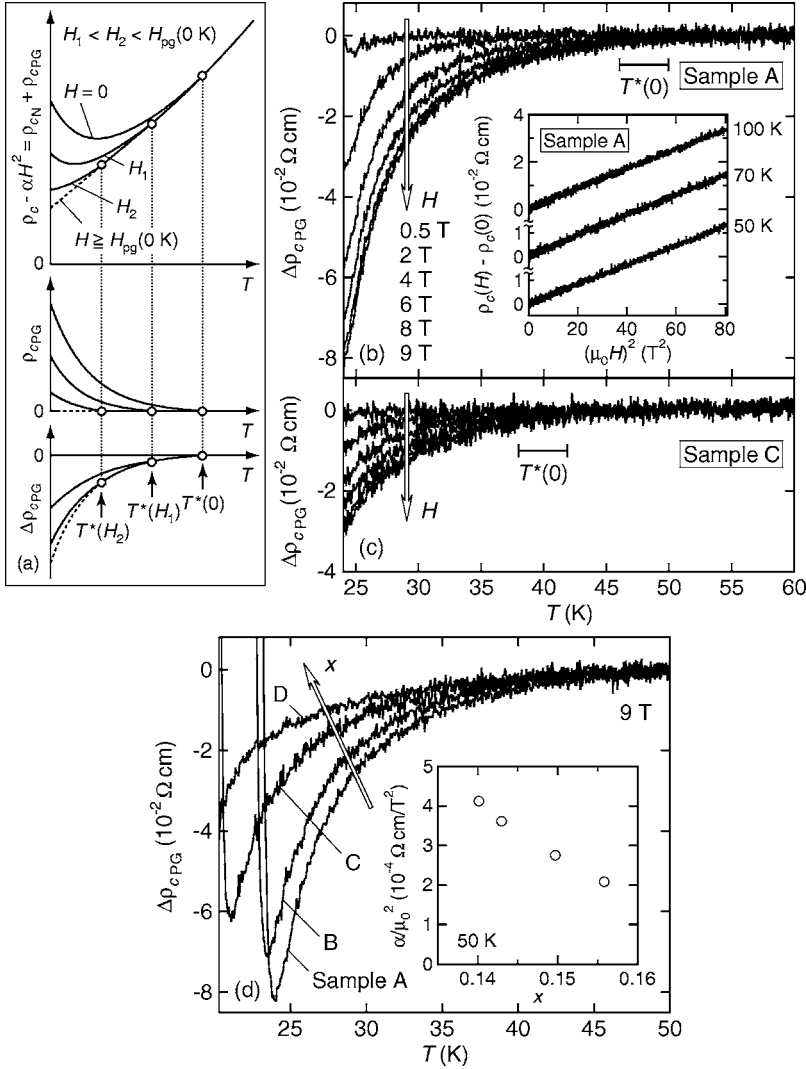
FIG. 5. (a) Schematic illustration of $\rho_c - \alpha H^2$, ρ_{cPG}, and $\Delta\rho_{cPG}$ as a function of T, showing diminishing ρ_{cPG} and a shift of T^* with increasing H. (b),(c) T dependence of $\Delta\rho_{cPG} = \rho_c(T,H) - \rho_c(T,0) - \alpha(50\ \text{K})H^2$ for sample A and C. (d) $\Delta\rho_{cPG} - T$ at 9 T for samples A–D. Inset to (b): $\Delta\rho_c(H) - H^2$ for sample A at 50, 70, and 100 K. Inset to (d): Plots for α/μ_0^2 vs x at 50 K.

in $|R_H|$ in the superconducting region, where R_H is the Hall coefficient.[18,23] This understanding is based on the concept that the interlayer magnetotransport is related to the in-plane transport in the case of coherent tunneling.[24]

Above T^*, ρ_c is represented by $\rho_{cN} + \alpha H^2$ since the pseudogap is absent. Below T^*, on the other hand, the negative MR component $\Delta\rho_{cPG}$ evolves, which is expressed as $\Delta\rho_{cPG}(T,H) = \rho_{cPG}(T,H) - \rho_{cPG}(T,0) = \rho_c(T,H) - \rho_c(T,0) - \alpha(T)H^2$, and illustrated in Fig. 5(a). Figure 5(b) shows the T dependences of $\Delta\rho_{cPG}$ at different fields for sample A. It is seen that the $\Delta\rho_{cPG}$-T curves obtained at different fields collapse on a single line above 48 ± 2 K while they starts to deviate below 48 ± 2 K. From this, we determine the zero-field T^* value to be 48 ± 2 K for sample A. The error involved in this determination of T^* is clearly no greater than ±2 K. Similarly, we obtain values of $T^* = 45$, 40, and 35 K for samples B, C, and D, respectively. The $\Delta\rho_{cPG}$-T curve for sample C is also shown in Fig. 5(c) to make clear the shift of T^* at different x. Figure 5(d) shows $\Delta\rho_{cPG}(T)$ at 9 T for samples A–D. The negative MR, i.e., $\Delta\rho_{cPG}$, is seen to decrease with doping, which is the result consistent with Figs. 4(c)–4(f). The large difference of $\Delta\rho_{cPG}$ around 25 K among samples A–D mainly comes from the difference in T^*, as seen in Figs. 5(b) and 5(c).

The value for T^* in the presence of a magnetic field H is obtained from the difference between the $\Delta\rho_{cPG}(H)$-T curve and another curve under a higher magnetic field, as depicted in Fig. 5(a). As a case of $\mu_0 H = 6$ T for sample A, the T dependence of $\Delta\rho_{cPG}(H) - \Delta\rho_{cPG}(6\ \text{T})$ for $\mu_0 H = 8$ and 9 T is shown in Fig. 6(a). The curves start to deviate from 0 at $T \simeq 40$ K so that we obtain a value of $T^*(6\ \text{T}) = 40\pm2$ K, which is lower than $T^*(0)$ by approximately 8 K. This definitely indicates that T^* depends on the magnetic field notably and so does the pseudogap. To check the validity of this evaluation, the ρ_c-H curve at 40 K is depicted in Fig. 6(b) together with the curve of $\rho_{cN}(40\ \text{K}) + \alpha(50\ \text{K})H^2$ for $\mu_0 H > 6$ T. It is clearly seen that both curves coincide for $\mu_0 H > 6$ T, implying that the pseudogap is absent for $\mu_0 H > 6$ T at 40 K. This is consistent with the result of $T^* = 40\pm2$ K at $\mu_0 H = 6$ T determined from the curves in Fig. 6(a). The other values are shown in Fig. 7(a) for samples A and B (Ref. 25).

IV. DISCUSSION

Figure 7(a) shows the x dependence of T_c and T^* obtained in the present study. Also plotted in Fig. 7(a) are the values
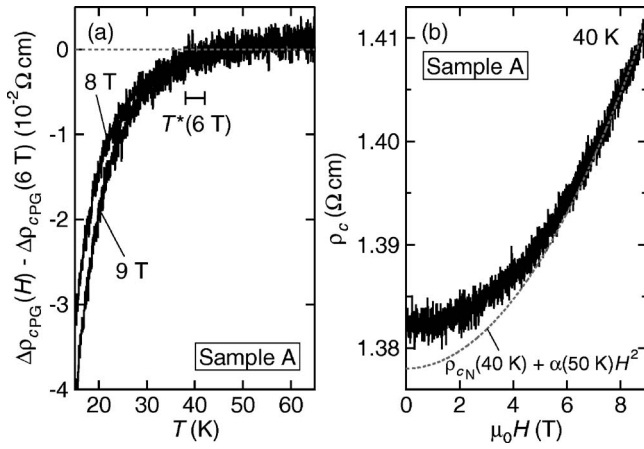
FIG. 6. (a) T dependence of $\Delta\rho_{cPG}(T,H) - \Delta\rho_{cPG}(T,6\ \text{T})$ at $\mu_0 H = 8$ and 9 T for sample A. (b) H dependence of ρ_c at 40 K for the same sample. The dashed line represents $\rho_{cN}(40\ \text{K}) + \alpha(50\ \text{K})H^2 = \rho_c(40\ \text{K}, 9\ \text{T}) - \alpha(50\ \text{K})(9/\mu_0)^2 + \alpha H^2$. Both curves coincide for $\mu_0 H > 6$ T, indicating consistency with $T^*(6\ \text{T}) = 40$ K.

for T^* obtained by Alff *et al.*[11] There are two characteristic features: (i) T^* decreases with doping monotonically and nearly linearly and (ii) T^* is higher than T_c in the whole doping range in the present study. These features are definite and remain unchanged even if a different definition is adopted for the determination of T^*, as is clear in Fig. 7(a), where the values for T^* determined by an extreme definition of $\Delta\rho_{cPG}(T^*) = -0.02\ \Omega\,\text{cm}$ are plotted as the lower bound for T^* in the present definition. Evidently, the present result is at variance with the tunneling spectroscopy results by Alff *et al.*,[11] in which T^* is lower than T_c and appears to vanish in the superconducting region. As revealed in the present study, T^* decreases with increasing magnetic field. In light of this field dependence of T^*, the values by Alff *et al.* can be smaller than the present values obtained in the absence of magnetic fields since their tunneling experiments were conducted in a magnetic field of $\mu_0 H = 14$ T. Therefore, values for T^* from Alff *et al.*, as plotted in Fig. 7, may be understood as an extension of our field-dependent T^* data, contrary to their postulation of the field independence of T^*.

When we take into account the carrier density for the n-type cuprates, as discussed later in this section, the doping levels of the present samples are considered to lie in the overdoped region. Therefore, the present result implies that T^* is observed even in the overdoped region. This is consistent with the recent result observed by Dagan *et al.*[12] in the electron-doped $\text{Pr}_{2-x}\text{Ce}_x\text{CuO}_4$, and the behavior of T^* is thought to be common in the n-type cuprates.

In the nonsuperconducting region, on the other hand, the pseudogap is observed at high energies.[6,8] Its onset temperature T^* decreases with x and disappears at around $x=0.14$ in the case of NCCO.[6] In the case of PCCO,[8] the pseudogap disappears near $x=0.16$ in the superconducting region, suggesting the existence of QCP. These results probably imply that the critical x at which T^* vanish depends on the kind of material. In the present study, the interlayer transport basically probes the zero-bias conductance so that, strictly speak-
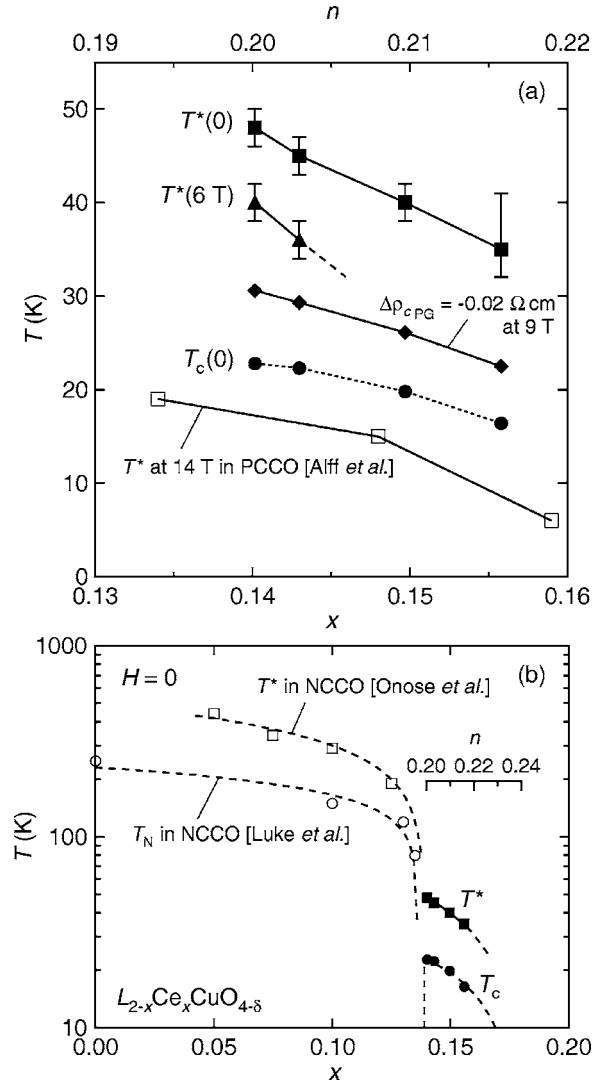

FIG. 7. (a) x dependence of $T^*(0)$, $T^*(6\ \text{T})$, T_c at $H=0$. Filled diamonds show the values for T^* obtained by an extreme definition of $\Delta\rho_{cPG} = -0.02\ \Omega\,\text{cm}$ at 9 T. These plots indicate the lower bound for the ambiguity associated with the arbitrariness of the definition of T^*, demonstrating that even in such a case it holds that $T^* > T_c$. The T^* values for PCCO obtained by Alff *et al.* (Ref. [11]) at 14 T are also plotted. The bars at the top indicates approximate values for n, the number of electrons per Cu site when $\delta = 0.03$. (b) The phase diagram for the n-type $L_{2-x}\text{Ce}_x\text{CuO}_{4-\delta}$ system on the semilogarithmic scale in the absence of a magnetic field. The values for T^* from the optical conductivity data (Ref. [6]) and the values for Néel temperature T_N by the muon spin rotation and relaxation measurements (Ref. [26]) for NCCO are used as the data for the antiferromagnetic region. The dashed lines are guides to the eyes.

ing, it is difficult to discern which pseudogap the present result is related to. Actually, however, the magnitude of T^* is used to estimate the magnitude of the pseudogap. In the present case, T^* is ~48 K so that the pseudogap is estimated to be of the order of less than 10 meV. Therefore, the pseudogap we have measured is clearly the low-energy pseudogap. Then the next interesting question is whether the large pseudogap is continuously connected to the small pseudogap near the antiferromagnetic phase boundary. At

present, it is probably understood that the large pseudogap is related to the (π, π) scattering of electrons, while the small pseudogap is ascribed to the fluctuation of superconductivity or of a different kind. Therefore, the high-energy pseudogap is likely to be different from the low energy pseudogap in origin. Then it follows that the observed sensitive change in T^* under a magnetic field is due to this nature of the low-energy pseudogap.

The Fermi-liquid-like resistive behavior and the monotonic decrease in T_c with parallel shift of the transition curve are reminiscent of characteristics observed in overdoped p-type cuprates.[27–29] The x and T dependence of H_{peak} show the tendency similar to that in overdoped BSCCO,[2] where the field-dependent T^* was also observed. If we allow for the value of $\delta \simeq 0.03$ from the oxygen-reducing condition[30] n, the number of electrons per Cu site, ranges from 0.20 to 0.22 for the mesas, as seen in Fig. 7. The present results imply that in the SCCO system the superconductivity appears in the overdoped region because the antiferromagnetic phase persists to a much higher doping level than in the p-type system.[31–33] Then the doping dependence of T^*, characterized both by a monotonic decrease with x and by a value much higher than T_c, can be viewed as a behavior observed in overdoped region. This behavior is qualitatively consistent with the experimental facts in overdoped BSCCO,[2,3] suggest-

ing that the pseudogap is likely to be of the same origin both for the n- and p-type high-T_c cuprates.

V. CONCLUSIONS

We have measured the interlayer transport by using the 30-nm-thick small mesa structures for superconducting n-type SCCO with various x. All the mesas exhibit ρ_c with a negative MR component, from which T^* is determined. At a doping level of $x \sim 0.140$, which is close to the phase boundary between superconductivity and antiferromagnetism, T^* is found to be as low as 48 K. It is also found that T^* decreases linearly with increasing x, while it keeps a value higher than T_c. For all the samples, the transport characteristics are reminiscent of those for overdoped p-type cuprates. These results suggest that the phase diagram for the pseudogap in the SCCO system is primarily similar to that in the p-type cuprates.

ACKNOWLEDGMENTS

*Electronic address: tsuyoshi@sk.kuee.kyoto-u.ac.jp

†Department of Physics, Kyoto University, Sakyo-ku, Kyoto 606-8502, Japan

[1] T. Timusk and B. Statt, Rep. Prog. Phys. **62**, 61 (1999).

[2] T. Shibauchi, L. Krusin-Elbaum, M. Li, M. P. Maley, and P. H. Kes, Phys. Rev. Lett. **86**, 5763 (2001).

[3] K. Anagawa, T. Watanabe, and M. Suzuki, Phys. Rev. B **73**, 184512 (2006).

[4] N. P. Armitage, D. H. Lu, C. Kim, A. Damascelli, K. M. Shen, F. Ronning, D. L. Feng, P. Bogdanov, Z.-X. Shen, Y. Onose, Y. Taguchi, Y. Tokura, P. K. Mang, N. Kaneko, and M. Greven, Phys. Rev. Lett. **87**, 147003 (2001).

[5] N. P. Armitage, F. Ronning, D. H. Lu, C. Kim, A. Damascelli, K. M. Shen, D. L. Feng, H. Eisaki, Z.-X. Shen, P. K. Mang, N. Kaneko, M. Greven, Y. Onose, Y. Taguchi, and Y. Tokura, Phys. Rev. Lett. **88**, 257001 (2002).

[6] Y. Onose, Y. Taguchi, K. Ishizaka, and Y. Tokura, Phys. Rev. Lett. **87**, 217001 (2001).

[7] Y. Onose, Y. Taguchi, K. Ishizaka, and Y. Tokura, Phys. Rev. B **69**, 024504 (2004).

[8] A. Zimmers, J. M. Tomczak, R. P. S. M. Lobo, N. Bontemps, C. P. Hill, M. C. Barr, Y. Dagan, R. L. Greene, A. J. Millis, and C. C. Homes, Europhys. Lett. **70**, 225 (2005).

[9] A. Koitzsch, G. Blumberg, A. Gozar, B. S. Dennis, P. Fournier, and R. L. Greene, Phys. Rev. B **67**, 184522 (2003).

[10] G. Q. Zheng, T. Sato, Y. Kitaoka, M. Fujita, and K. Yamada, Phys. Rev. Lett. **90**, 197005 (2003).

[11] L. Alff, Y. Krockenberger, B. Welter, M. Schonecke, R. Gross, D. Manske, and M. Naito, Nature (London) **422**, 698 (2003).

[12] Y. Dagan, M. M. Qazilbash, and R. L. Greene, Phys. Rev. Lett.

94, 187003 (2005).

[13] S. Kleefisch, B. Welter, A. Marx, L. Alff, R. Gross, and M. Naito, Phys. Rev. B **63**, 100507(R) (2001).

[14] T. Kawakami, T. Shibauchi, Y. Terao, M. Suzuki, and L. Krusin-Elbaum, Phys. Rev. Lett. **95**, 017001 (2005).

[15] M. Suzuki, T. Watanabe, and A. Matsuda, Phys. Rev. Lett. **82**, 5361 (1999).

[16] T. Watanabe, T. Fujii, and A. Matsuda, Phys. Rev. Lett. **84**, 5848 (2000).

[17] P. K. Mang, S. Larochelle, A. Mehta, O. P. Vajk, A. S. Erickson, L. Lu, W. J. L. Buyers, A. F. Marshall, K. Prokes, and M. Greven, Phys. Rev. B **70**, 094507 (2004).

[18] Y. Hidaka and M. Suzuki, Nature (London) **338**, 635 (1989).

[19] J. L. Peng, Z. Y. Li, and R. L. Greene, Physica C **177**, 79 (1991).

[20] M. Suzuki, T. Watanabe, and A. Matsuda, Phys. Rev. Lett. **81**, 4248 (1998).

[21] L. Krusin-Elbaum, G. Blatter, and T. Shibauchi, Phys. Rev. B **69**, 220506(R) (2004).

[22] H. Kontani, J. Phys. Soc. Jpn. **70**, 1873 (2001).

[23] J. M. Harris, Y. F. Yan, P. Matl, N. P. Ong, P. W. Anderson, T. Kimura, and K. Kitazawa, Phys. Rev. Lett. **75**, 1391 (1995).

[24] N. Kumar and A. M. Jayannavar, Phys. Rev. B **45**, 5001 (1992).

[25] For sample C and D, $T^*(6\ \text{T})$ was not able to be determined because the $\rho_{cPG}(H)$ data was small and led to undulation after subtraction, which made it difficult to determine the temperature at which the curve deviates from 0. This is probably caused by the error in the estimation of α, which can be temperature-dependent sightly.

[26] G. M. Luke, L. P. Le, B. J. Sternlieb, Y. J. Uemura, J. H. Brewer, R. Kadono, R. F. Kiefl, S. R. Kreitzman, T. M. Riseman, C. E.

Stronach, M. R. Davis, S. Uchid, H. Takagi, Y. Tokura, Y. Hidaka, T. Murakami, J. Gopalakrishnan, A. W. Sleight, M. A. Subramanian, E. A. Early, J. T. Markert, M. B. Maple, and C. L. Seamanz, Phys. Rev. B **42**, 7981 (1990).

[27] M. Suzuki and M. Hikita, Phys. Rev. B **44**, 249 (1991).

[28] Y. Nakamura and S. Uchida, Phys. Rev. B **47**, R8369 (1993).

[29] A. P. Mackenzie, S. R. Julian, G. G. Lonzarich, A. Carrington, S. D. Hughes, R. S. Liu, and D. C. Sinclair, Phys. Rev. Lett. **71**, 1238 (1993).

[30] T. Kawashima and E. Takayama-Muromachi, Physica C **219**, 389 (1994), in this reference, a δ of 0.02 to 0.03 gives the highest T_c. The oxygen reduction condition in the present study is rather close to the one that gave $\delta=0.03$ in Ref. 30 so that we adopted $\delta=0.03$ to estimate vales of n.

[31] For T'-type $La_{2-x}Ce_xCuO_4$ thin films, the underdoped regime is located for $x<0.09$ because of a narrower antiferromagnetic region (Ref. 32). In SCCO, a wider antiferromagnetic region is probably caused by a small ionic radius of Sm (Ref. 33).

[32] M. Naito and M. Hepp, Jpn. J. Appl. Phys., Part 2 **39**, L485 (2000).

[33] M. Fujita, T. Kubo, S. Kuroshima, T. Uefuji, K. Kawashima, K. Yamada, I. Watanabe, and K. Nagamine, Phys. Rev. B **67**, 014514 (2003).